Phase control of plasmon enhanced two-photon photoluminescence in resonant gold nanoantennas

Phase control of plasmon enhanced two-photon photoluminescence in resonant gold nanoantennas

Vikas Remesh,[1] Michael Stührenberg,[2] Lisa Saemisch,[1] Nicolò Accanto,[1,a)] and Niek F. van Hulst[1,3,b)]
[1]*ICFO—Institut de Ciences Fotoniques, The Barcelona Institute of Science and Technology, 08860 Castelldefels, Barcelona, Spain*
[2]*Department of Physics, Chalmers University of Technology, SE-412 96 Gothenburg, Sweden*
[3]*ICREA—Institució Catalana de Recerca i Estudis Avançats, 08010 Barcelona, Spain*

(Received 8 August 2018; accepted 23 October 2018; published online 20 November 2018)

Plasmonic nanoantennas emit two-photon photoluminescence, which is much stronger than their second harmonic generation. Unfortunately, luminescence is an incoherent process and therefore generally not explored for nanoscale coherent control of the antenna response. Here, we demonstrate that, in resonant gold nanoantennas, the two-photon absorption process can be coherent, provided that the excitation pulse duration is shorter than the dephasing time of plasmon mode oscillation. Exploiting this coherent response, we show the pure spectral phase control of resonant gold nanoantennas, with effective read-out of the two-photon photoluminescence. https://doi.org/10.1063/1.5051381

Metal nanostructures driven at optical frequency display coherent charge density oscillations of conduction electrons: plasmon modes with resonances determined by the dispersion, shape, and size of the nanostructure. The plasmon resonances concentrate the electromagnetic field in subwavelength hotspots, which is widely explored to enhance the fluorescence[1–3] and Raman scattering response of molecules.[4,5] The nanostructures emit the enhanced response with modified rates and in specific directions, thus acting as true nanoantennas. Beyond an enhanced amplitude, the electromagnetic field of the antenna resonance exhibits an intrinsic phase response, in space and time.[6] The subwavelength amplitude-phase feature allows the nanoscale coherent control of the nanoantenna and manipulation of the light-matter interaction at the nanoscale, to boost non-linear processes for the development of nanoscale devices. Unfortunately, owing to intrinsic metal losses, it is challenging to observe the coherent response of plasmons, as they are typically short-lived. The typical dephasing times for Au and Ag nanostructures vary from below 10 fs to few tens of femtoseconds.[7,8]

In pioneering theoretical papers, Stockman and coworkers[9,10] proposed the use of tailored phase modulation of excitation femtosecond pulses to control the spatial distribution of optical fields in nanostructures, provided that the excitation time is ensured to be shorter than the dephasing time. Aeschliman *et al.*[11] showed the control of the optical near field in the vicinity of silver nanostructures by means of two photon Photo-Emission Electron Microscopy (PEEM) and adaptive modulation of the excitation polarisation of femtosecond pulses.

For the best performance of a nanoscale plasmonic device, an all-optical control scheme is preferred. The control of light with light, exploiting nanostructures as a platform, has been shown by many groups. For example, Novotny and coworkers[12] proposed the control of intensity and direction of scattered light from a nanowire by adjusting the coherent interaction between the polarization currents generated by linear and second harmonic scattering. Sukharev and Seideman,[13] showed the control of energy transport in a chain-structure of nanoparticles, adjusting polarization and phase between transverse and longitudinal plasmonic modes, while Papoff *et al.*[14] proposed to use the phase between the excitation field and the generated multiphoton signal to control absorption and scattering in nanospheres. Following the early proposal by Stockman and co-workers[9,10] several groups modelled the response of nanoparticles to ultrafast broadband lasers. Gray and coworkers[15] calculated the spatiotemporal control of localised electromagnetic field hotspots on nanowire and nanocone systems with respect to the sign of the chirp of excitation laser pulses. Scherer and coworkers[16] demonstrated the generation, control, and focussing of plasmonic wave packets in silver nanowire systems, while Hecht and coworkers[17] calculated the deterministic spatiotemporal control of nano-optical fields in two wire plasmonic nanocircuits and asymmetric nanoantennas. The first ultrafast experimental optical coherent control was presented by Kubo *et al.*[18] showing spatiotemporal dynamics of propagating plasmons at the sub-femtosecond timescale using PEEM for nanoscale imaging, a technique picked up by several others.[19–21] The Zentgraf group[22] showed an all-optical control of a coupled plasmonic structure, controlling the phase between two competitive channels. Recently, the Lienau group[23] presented broad-band spectral interferometry at different spatial positions of a slit-groove structure to reconstruct the dispersion of the surface plasmon upon propagation. The Imura group[24] demonstrated plasmonic wavepacket interference of two simultaneously launched higher-order plasmon modes in a long gold nanorod, using ultrafast near field microscopy, and they reported local variation of intensity on a rough gold film,

a)Present address: Neurophotonics Laboratory, Paris Descartes University, Paris, France.
b)E-mail: Niek.vanHulst@ICFO.eu.

due to interference of local excitations by control of the linear phase modulation of the excitation pulses.[25] Yet despite progress on detection and control of phase on propagation, a systematic, true optical coherent control on a fundamental dipole plasmon mode remains challenging due to the very short dephasing time of the plasmon oscillation in the 25 fs range. In this work, we address this ultrashort timescale demonstrating the coherent response. Next, we show the development of the plasmonic phase control while extending from short to longer timescales beyond the dephasing time.

In the optical domain, both second harmonic generation (SHG) and two-photon photoluminescence (TPPL) are widely used non-linear responses to characterize the resonant plasmon modes in nanoantennas. Although intrinsically coherent, the SHG response of individual nanoantennas is usually weak, which makes it challenging to perform phase control by detecting SHG on single nanoantennas. On the contrary, the incoherent TPPL response is one to two orders of magnitude stronger than SHG. It is well-known that the strong local field enhancement due to resonances contributes to the enhanced TPPL.[26–28] Thus, TPPL is a very suitable non-linear optical read-out method to probe nanoscale responses.

We investigated the time and phase response of TPPL of Au nanoantennas. An array of Au nanoantennas (each 50 nm in width, 50 nm in height, and length increasing from 50 nm to 300 nm) were fabricated with electron beam lithography on a glass coverslip with a 10 nm thin indium tin oxide adhesion layer. As a reference, we detected the SHG response of commercially available non-resonant BaTiO3 nanoparticles (Sigma-Aldrich), dissolved in ethanol and drop-casted on a coverslip to obtain sparsely distributed nanoparticles on an area. The excitation source was a broadband titanium-sapphire laser (Octavius 85M, Menlo Systems) with a bandwidth of ~100 nm and a Fourier-limited pulse duration of 10 fs at a central wavelength of 790 nm. The experimental setup is sketched in Fig. 1(a). The laser excites individual nanoparticles at the focus of a high numerical aperture objective (Zeiss Axiovert 200, Zeiss Plan Apochromat 100× 1.46 Oil Objective). An avalanche photodiode (APD) or a spectrometer equipped with an electron multiplying CCD camera (Andor) collects the TPPL/SHG signal. A 4f pulse shaper in folded geometry equipped with a spatial light modulator (640 pixels, CRi, adapted from MIIPS box, Biophotonics Solutions, Inc.) exerts the spectral phase control. A MIIPS pulse compression scheme, detecting SHG of $BaTiO_3$ nanoparticles at the microscope focus (procedure described elsewhere[28]), is applied to ensure that the laser pulses are free of phase distortion in the excitation confocal volume.

First, to identify the nanoantenna resonance, an Au nanoantenna sweep array (50–300 nm in length) was imaged, with the exciting laser polarized linearly along the long axis of the individual nanoantennas, at an average power of 60 kW/cm^2 in the diffraction-limited spot, collecting the spectrally integrated TPPL signal in the epi-fluorescence mode with 670 and 680 nm short-pass in front of the APD. We used a 458 nm long-pass filter to make sure that we reject the contribution of SHG. Figure 1(b) shows the TPPL image of the 50 μm × 50 μm nanoantenna array. We find that for the 790 nm central wavelength, the resonant Au nanoantenna length is 140 nm, with a length

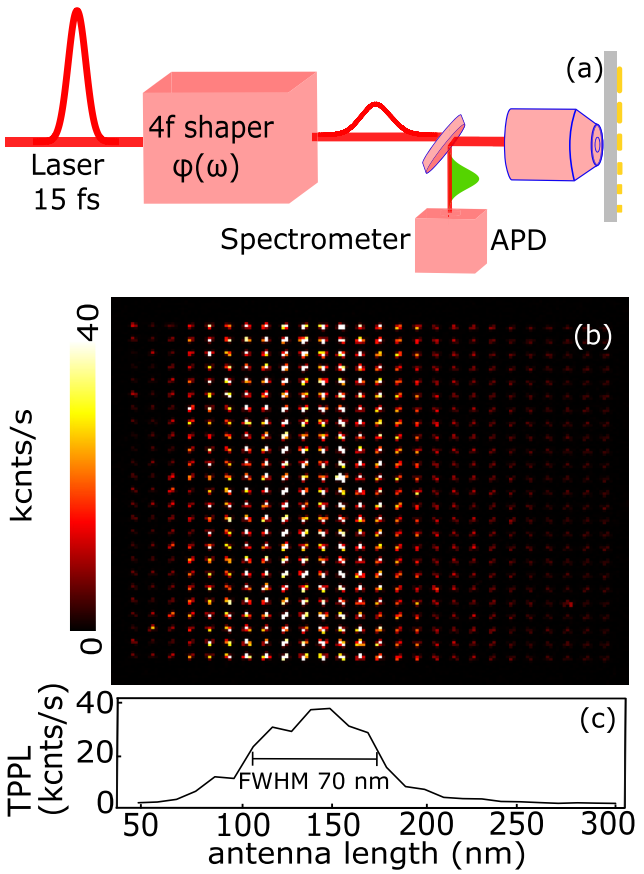

FIG. 1. Tuning the antenna resonance: (a) 15 fs pulses from a Ti:S laser are shaped with a 4f shaper and directed to the confocal sample scanning microscope. The two-photon response of a chosen antenna in an array is collected in the epi-confocal mode with a photocounting avalanche photodiode (APD) or spectrometer. (b) TPPL image of an array of Au nanoantennas with the increasing length from 50 nm to 300 nm. (c) TPPL response shows the dipole resonance at an antenna length of 140 nm.

distribution of ~70 nm (FWHM) [Fig. 1(c)], in agreement with theory and earlier reports.[27]

Next, to investigate the power dependence of the TPPL, we measured the two-photon emission spectra in the spectral range of 370–650 nm, as the excitation power of the Fourier limited pulse was varied from 0 to 60 kW/cm^2 (average power). The line plot in Fig. 2(a) shows the full TPPL spectrum of a single resonant Au nanoantenna. One can also identify the weak and narrow SHG spectrum in the range of 370 nm–440 nm. Subsequently, we built a complete two-photon power spectrogram, average of many measurement cycles, which shows the evolution of the spectral response of both SHG and TPPL with the variation in excitation power [Fig. 2(b)]. To derive the power dependence, the collected spectrograms were fit with a power law $I_{out} = aI_{in}^b$, where I_{in} and I_{out} are the input and output powers, respectively, with a spectral resolution of 6 nm. Figure 2(c) shows the fitted values of the power law exponent b as a function of the detected wavelength. The plot confirms the strict quadratic power dependence of SHG spectral response. The average power dependence of the TPPL is $b = 2.25$, which confirms that the TPPL is dominated by two-photon absorption, with only minor contributions from higher order absorption processes.

Next, we investigate the phase response of the TPPL. We start with a basic phase control experiment: increasing

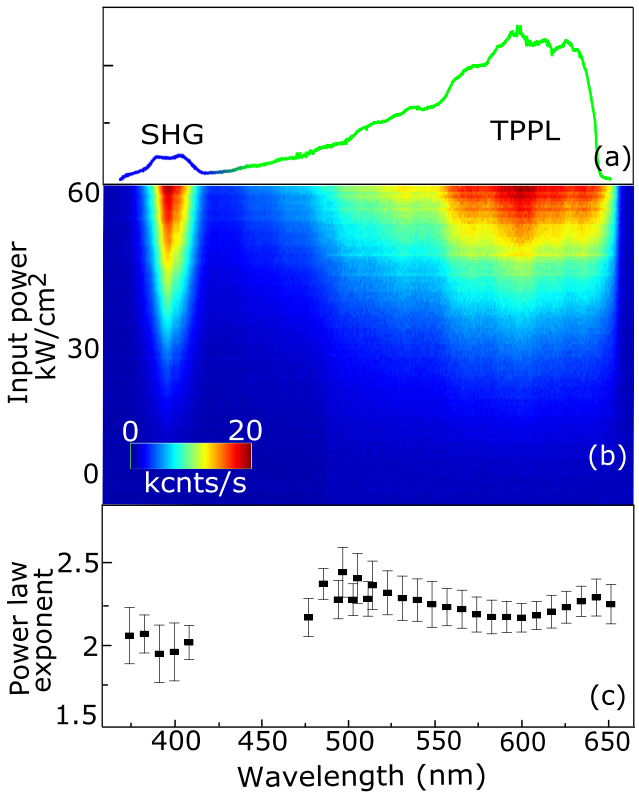

FIG. 2. Nonlinear optical response of a resonant antenna. (a) Two-photon spectrum of a nanoantenna showing the spectral range of SHG and TPPL. (b) Evolution of the full two-photon spectrum for a sweep of input power from 0 to 60 kW/cm^2. (c) Spectrally resolved fit values for the power law exponent shows that the SHG is strictly quadratic, while the TPPL is slightly higher with an average power dependence of 2.25.

the second order dispersion of the excitation laser pulse from its shortest possible duration—the transform limit—to a given longer pulse duration and collecting the corresponding two-photon signal. The spectral phase of a broadband laser is generally written as a Taylor series with respect to the central frequency ω_0 of the laser

$$\varphi = \varphi^{(0)} + \varphi^{(1)}(\omega - \omega_0) + \frac{1}{2}\varphi^{(2)}(\omega - \omega_0)^2 \cdots, \quad (1)$$

where $\varphi^{(0)}$ gives the absolute phase of the laser pulse envelope, $\varphi^{(1)}$ gives the linear phase, and $\varphi^{(2)}$ gives the magnitude of the quadratic variation of the spectral phase of any given frequency component ω in reference to ω_0. The first term is the absolute phase, while the second term, in the time domain, allows controlling the delay between the frequency components with respect to ω_0. Both have no effect on the temporal properties of the pulse, and hence, we concentrate on the quadratic phase term $\varphi^{(2)}$, also called the second order dispersion. A positive value of $\varphi^{(2)}$ implies that in the time domain, the frequency increases with time and that the "blue" components of the spectrum come after the "red" components and a negative value implies vice versa. Also, with a given magnitude of the second order dispersion, the temporal width of the pulse changes, and from the Fourier relations, it can be shown that, for a transform limited laser pulse length τ, with a Gaussian spectral profile, for a given $\varphi^{(2)}$, the resulting pulse duration τ_{out} is given by

$$\tau_{out}^2 = \tau^2 + \left(4ln2\frac{\varphi^{(2)}}{\tau}\right)^2. \quad (2)$$

It has to be noted that, in our experiment, following the pulse compression, the "compensation phase mask" applied will result in a nearly zero phase across the full excitation laser spectral range for diffraction-limited laser pulse at the sample volume.[28] Controlled second order dispersion was then sequentially added on top of this compensation spectral phase by sending appropriate voltage masks to the spatial light modulator. In our measurements, we used 301 phase masks with $\varphi^{(2)}$ from 0 to 5000 fs^2 keeping the pulse energy constant. First, we performed this second order dispersion scan on the $BaTiO_3$ nanoparticle reference sample, detecting the SHG response. We chose the $BaTiO_3$ nanoparticle as it is non-resonant within our laser spectral range, and hence, the particle phase has no effect on the spectral phase of the excitation laser field and the particle is not affected by resonant spectral narrrowing.[6,28] Figure 3 shows that the SHG response with respect to pulse duration is proportional to τ^{-1}, as expected for a two-photon coherent process and constant pulse energy.[29,30] A similar pulse stretch measurement on TPPL of Au nanoantennas shows a peculiar response. We observe that for long pulses, the TPPL response decreases proportional to τ^{-1} similar to the SHG. At shorter pulses, the TPPL deviates to a plateau around ~500 fs pulse length. A similar plateau was observed by Biagioni and coworkers[31,32] for pulse duration $\tau < 1$ ps and was attributed to the lifetime of the intermediate state involved in the sequential $1+1$ photon absorption mechanism observed in gold nanostructures.[26] However, here beyond the plateau, we observe a ~77% increase in TPPL intensity as the pulse duration is further shortened from 100 fs down to 15 fs. The TPPL is dominated by quadratic power response, and thus, higher order multiphoton absorption cannot explain this increase for short pulses. We attribute the increase in TPPL response in the very short pulse duration regime to the contribution of

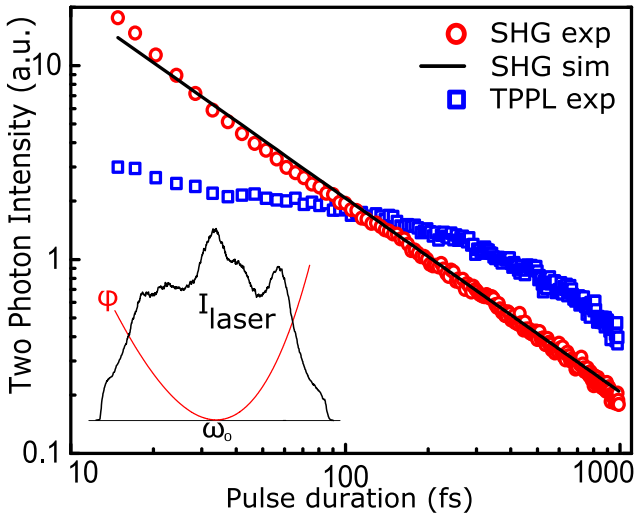

FIG. 3. Response on extending the pulse duration. Two-photon response with the increasing excitation pulse duration for SHG and TPPL. The SHG decreases with a slope of −1. In contrast, the TPPL exhibits a plateau for short pulses. The inset shows the laser spectrum and the quadratic spectral phase applied to stretch the laser pulse from its Fourier limit.

coherent plasmon oscillations, as the onset of the coherent τ^{-1} response, which becomes relevant on these timescales. Our experiment suggests that TPPL, regarded as an incoherent process, develops a phase response on the timescales faster than the dephasing of the plasmon resonance. We verify this by pure phase control.

Finally, we perform a phase control experiment on the TPPL response, within the plasmon dephasing time. A coherent two-photon excitation is readily turned from constructive into destructive interference by a π-phase flip in one of the two excitation steps. With this in mind, we added a static π-phase step at the central frequency ω_0 in the laser spectrum, in addition to the second order dispersion. In fact, such a π–phase step has been previously used to effectively control various nonlinear optical processes in various systems.[33] The combination of the π step and $\varphi^{(2)}$ means that, in addition to the excitation pulses getting stretched temporally, there is a π phase difference between blue and red halves of the laser spectrum, i.e., between the collective two-photon pairs contributing to the two-photon absorption process. Any phase response that exists depending on the excitation pulse duration would reveal its signature on applying such a spectral π-step. The spectral π-phase step is defined as $\varphi_\pi = \frac{\pi}{2} sign(\Omega)$, where $\Omega = \omega - \omega_0$ and $sign(\Omega)$ takes values -1 and $+1$ with respect to ω_0. The sum of [Eq. (1)] and the step-function will then form the effective phase mask for this experiment. In the spectral domain, the SHG spectrum $S(2\omega)$ can be calculated by convoluting the excitation spectrum against itself, spread over the entire two-photon spectral range

$$S(2\omega) = \left| \int |E(\omega_0 + \Omega)||E(\omega_0 - \Omega)| \times \exp\{i[\varphi(\omega_0 + \Omega) + \varphi(\omega_0 - \Omega)]\} d\Omega \right|^2 . \quad (3)$$

With the effective phase inserted into Eq. (3), the SHG spectrum $S(2\omega)$ is given by

$$S(2\omega) = \left| \int |E(\omega_0 + \Omega)||E(\omega_0 - \Omega)| \times \exp\left\{ i\left[\frac{\varphi^{(2)}}{2}(\Omega)^2 + \frac{\pi}{2} sign(\Omega) \right] \right\} d\Omega \right|^2 . \quad (4)$$

From Eq. (4), the integrated intensities I for varying $\varphi^{(2)}$ and $\varphi^{(2)} + \varphi_\pi$ can be deducted. We define the relative difference between $I_{\varphi^{(2)}}$ and $I_{\varphi^{(2)}+\varphi_\pi}$, the intensities using chirped laser pulses with and without a π step mask, respectively, as the coherent contrast β as follows:

$$\beta = \frac{I_{\varphi^{(2)}} - I_{\varphi^{(2)}+\varphi_\pi}}{I_{\varphi^{(2)}}} . \quad (5)$$

We then determine the TPPL phase response on resonant Au nanoantennas of 140 nm length and compare to the SHG reference on the non-resonant $BaTiO_3$ nanoparticles. The π step was fixed at 790 nm, the central frequency (ω_0) of our laser spectrum. We varied the second order dispersion from 0 to 2000 fs^2. Figure 4 shows the results. For SHG, at the Fourier limit with $\varphi^{(2)} = 0$, the coherent contrast β is 56% and as the

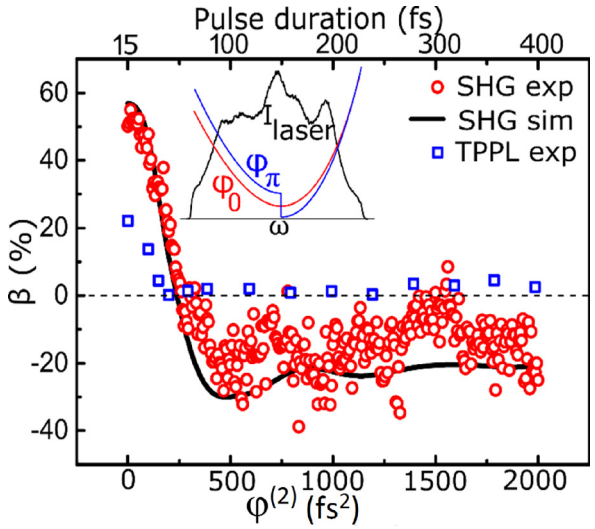

FIG. 4. The coherent contrast β of TPPL and SHG on extending the pulse duration. The TPPL contrast decreases and reaches zero at a second order dispersion of 200 fs^2, which is around 50 fs pulse duration. The SHG shows strong contrast for any pulse length and cross zero at 250 fs^2. The inset shows the spectral phase of a simple quadratic phase (φ_0) and with a spectral π phase step on top of it (φ_π).

second order dispersion is increased, β drops until it crosses the zero level for $\varphi^{(2)} = 250$ fs^2. This means that for a particular value of $\varphi^{(2)}$, the effective integrated SHG signal detected does not recognise the difference between $\varphi^{(2)}$ and $\varphi^{(2)}+\varphi_\pi$; the second order dispersion cancels the effect of the π step. We define this phase as the crossover phase φ_c. From this zero crossing point, as we go increasing $\varphi^{(2)}$ further, β flips its sign. One notices that, beyond φ_c, the β value stays relatively constant at $\sim -20\%$ with a slight oscillatory trend. The experimental data nicely agree with the calculated expected response of SHG. In general, φ_c will also depend on the position of the step function in the laser spectrum. The most interesting observation here is the difference in β between TPPL and SHG. At the transform limit, β_{TPPL} is $\sim 25\%$, non-zero and about half of β_{SHG}. Thus, the TPPL does respond to pure phase control, confirming the coherent nature of the short-pulse onset observed in Fig. 3. On increasing $\varphi^{(2)}$, β_{TPPL} diminishes rapidly, to reach zero at ~ 200 fs^2, corresponding to an ~ 50 fs pulse length, and maintains at zero for longer pulses. This clearly demonstrates the differences in the coherent response between TPPL and SHG. TPPL shows coherent response on a very short timescale within the decoherence time, until which the plasmon oscillations preserve some phase memory. Beyond 50 fs, the temporal length of the excitation laser pulse becomes unable to coherently drive the plasmon oscillations. We modelled this response, introducing a decoherence term into Eq. (4), to take into account the dephasing time of the plasmons in the gold. From the fit to the data in Fig. 4, we extracted a decoherence time of ~ 30 fs, which is of the same order of the values reported in the literature in similar systems.[7,8] Beyond this timescale, the two-photon excitation process in Au nanoantennas becomes dominated by the intermediate state dynamics, which has a lifetime of ~ 600 fs.[31,34]

We have presented the pure phase control of the nonlinear response of a resonant gold nanoantenna. By

combining the quadratic chirp phase and the π-step phase on a 10 fs Fourier-limited pulse, it is possible to distinguish and differentiate a true coherent process from a time-dependent coherent process. We show that the broad-band two-photon photoluminescence can be coherently excited and controlled by the spectral phase, provided that the excitation pulse is short enough compared to the plasmon mode decoherence time of $\sim$30 fs. Our method is effective to determine dephasing times and phase control contrast in nanoplasmonic systems, with application in nanoparticle labelled two-photon imaging.

The authors thank Richard Lane and Matz Liebel for assistance and advice on the pulse shaping. V.R. received support from the European Commission through the Erasmus Mundus Joint Doctorate Programme Europhotonics (Grant No. 159224-1-2009-1-FR-ERA MUNDUS-EMJD). N.F.v.H. acknowledges the financial support by the European Commission (ERC Advanced Grant No. 670949-LightNet), Spanish Ministry of Economy ("Severo Ochoa" program for Centres of Excellence in R&D SEV-2015-0522, PlanNacional FIS2015-69258-P and Network FIS2016-81740-REDC), the Catalan AGAUR (No. 2017SGR1369), Fundacio´ Privada Cellex, Fundacio´ Privada Mir-Puig, and Generalitat de Catalunya through the CERCA Program.

[1]A. Kinkhabwala, Z. Yu, S. Fan, Y. Avlasevich, K. Müllen, and W. E. Moerner, "Large single-molecule fluorescence enhancements produced by a bowtie nanoantenna," Nat. Photonics **3**, 654 (2009).
[2]P. Anger, P. Bharadwaj, and L. Novotny, "Enhancement and quenching of single-molecule fluorescence," Phys. Rev. Lett. **96**, 113002 (2006).
[3]S. Kühn, U. Håkanson, L. Rogobete, and V. Sandoghdar, "Enhancement of single-molecule fluorescence using a gold nanoparticle as an optical nanoantenna," Phys. Rev. Lett. **97**, 017402 (2006).
[4]K. Kneipp, Y. Wang, H. Kneipp, L. T. Perelman, I. Itzkan, R. R. Dasari, and M. S. Feld, "Single molecule detection using surface-enhanced Raman scattering (SERS)," Phys. Rev. Lett. **78**, 1667 (1997).
[5]S. Nie and S. R. Emory, "Probing single molecules and single nanoparticles by surface-enhanced Raman scattering," Science **275**, 1102 (1997).
[6]N. Accanto, L. Piatkowski, J. Renger, and N. F. van Hulst, "Capturing the optical phase response of nanoantennas by coherent second-harmonic microscopy," Nano Lett. **14**, 4078 (2014).
[7]A. Anderson, K. S. Deryckx, X. G. Xu, G. Steinmeyer, and M. B. Raschke, "Few-femtosecond plasmon dephasing of a single metallic nanostructure from optical response function reconstruction by interferometric frequency resolved optical gating," Nano Lett. **10**, 2519 (2010).
[8]T. Zhao, J. W. Jarrett, J. S. Johnson, K. Park, R. A. Vaia, and K. L. Knappenberger, Jr., "Plasmon dephasing in gold nanorods studied using single-nanoparticle interferometric nonlinear optical microscopy," J. Phys. Chem. C **120**, 4071 (2016).
[9]M. I. Stockman, S. V. Faleev, and D. J. Bergman, "Coherent control of femtosecond energy localization in nanosystems," Phys. Rev. Lett. **88**, 067402 (2002).
[10]M. I. Stockman, D. J. Bergman, and T. Kobayashi, "Coherent control of nanoscale localization of ultrafast optical excitation in nanosystems," Phys. Rev. B **69**, 054202 (2004).
[11]M. Aeschlimann, M. Bauer, D. Bayer, T. Brixner, F. J. G. de Abajó, W. Pfeiffer, M. Rohmer, C. Spindler, and F. Steeb, "Adaptive subwavelength control of nano-optical fields," Nature **446**, 301 (2007).
[12]S. G. Rodrigo, H. Harutyunyan, and L. Novotny, "Coherent control of light scattering from nanostructured materials by second-harmonic generation," Phys. Rev. Lett. **110**, 177405 (2013).
[13]M. Sukharev and T. Seideman, "Phase and polarization control as a route to plasmonic nanodevices," Nano Lett. **6**, 715 (2006).
[14]F. Papoff, D. Mcarthur, and B. Hourahine, "Coherent control of radiation patterns of nonlinear multiphoton processes in nanoparticles," Sci. Rep. **5**, 12040 (2015).
[15]T. W. Lee and S. K. Gray, "Controlled spatiotemporal excitation of metal nanoparticles with picosecond optical pulses," Phys. Rev. B **71**, 035423 (2005).
[16]L. Cao, R. A. Nome, J. M. Montgomery, S. K. Gray, and N. F. Scherer, "Controlling plasmonic wave packets in silver nanowires," Nano Lett. **10**, 3389 (2010).
[17]J. S. Huang, D. V. Voronine, P. Tuchscherer, T. Brixner, and B. Hecht, "Deterministic spatiotemporal control of optical fields in nanoantennas and plasmonic circuits," Phys. Rev. B **79**, 195441 (2009).
[18]A. Kubo, K. Onda, H. Petek, Z. Sun, Y. S. Jung, and H. K. Kim, "Femtosecond imaging of surface plasmon dynamics in a nanostructured silver film," Nano Lett. **5**, 1123 (2005).
[19]J. Lehmann, M. Merschdorf, W. Pfeiffer, A. Thon, S. Voll, and G. Gerber, "Surface plasmon dynamics in silver nanoparticles studied by femtosecond time-resolved photoemission," Phys. Rev. Lett. **85**, 2921 (2000).
[20]E. Mårsell, A. Losquin, R. Svard, M. Miranda, C. Guo, A. Harth, E. Lorek, J. Mauritsson, C. L. Arnold, H. Xu, A. L'Huillier, and A. Mikkelsen, "Nanoscale imaging of local few-femtosecond near-field dynamics within a single plasmonic nanoantenna," Nano Lett. **15**, 6601 (2015).
[21]Q. Sun, H. Yu, K. Ueno, A. Kubo, Y. Matsuo, and H. Misawa, "Dissecting the few-femtosecond dephasing time of dipole and quadrupole modes in gold nanoparticles using polarized photoemission electron microscopy," ACS Nano **10**, 3835 (2016).
[22]F. Zeuner, M. A. Muldarisnur, A. Hildebrandt, J. Förstner, and T. Zentgraf, "Coupling mediated coherent control of localized surface plasmon polaritons," Nano Lett. **15**, 4189 (2015).
[23]J.-M. Yi, D. Hou, H. Kollman, V. Smirnov, Z. Papa, P. Dombi, M. Silies, and C. Lienau, "Probing coherent surface plasmon polariton propagation using ultrabroadband spectral interferometry," ACS Photonics **4**, 347 (2017).
[24]Y. Nishiyama, K. Imura, and H. Okamoto, "Observation of plasmon wave packet motions via femtosecond time-resolved near-field imaging techniques," Nano Lett. **15**, 7657 (2015).
[25]K. Imaeda and K. Imura, "Optical control of plasmonic fields by phase-modulated pulse excitations," Opt. Express **21**, 27481 (2013).
[26]K. Imura, T. Nagahara, and H. Okamoto, "Near-field two-photon-induced photoluminescence from single gold nanorods and imaging of plasmon modes," J. Phys. Chem. B **109**, 13214 (2005).
[27]M. Castro-Lopez, D. Brinks, R. Sapienza, and N. F. van Hulst, "Aluminum for nonlinear plasmonics: Resonance-driven polarized luminescence of Al, Ag, and Au nanoantennas," Nano Lett. **11**, 4674 (2011).
[28]N. Accanto, J. B. Nieder, L. Piatkowski, M. Castro-Lopez, F. Pastorelli, D. Brinks, and N. F. van Hulst, "Phase control of femtosecond pulses on the nanoscale using second harmonic nanoparticles," Light: Sci. Appl. **3**, e143 (2014).
[29]C. Xu and W. W. Webb, "Measurement of two-photon excitation cross sections of molecular fluorophores with data from 690 to 1050 nm," J. Opt. Soc. Am. B **13**, 481 (1996).
[30]S. Tang, T. B. Krasieva, Z. Chen, G. Tempea, and B. J. Tromberg, "Effect of pulse duration on two-photon excited fluorescence and second harmonic generation in nonlinear optical microscopy," J. Biomed. Opt. **11**, 020501 (2006).
[31]P. Biagioni, M. Celebrano, M. Savoini, G. Grancini, D. Brida, S. Mátéfi-Tempfli, M. Mátéfi-Tempfli, L. Duò, B. Hecht, G. Cerullo, and M. Finazzi, "Dependence of the two-photon photoluminescence yield of gold nanostructures on the laser pulse duration," Phys. Rev. B **80**, 045411 (2009).
[32]P. Biagioni, D. Brida, J. S. Huang, J. Kern, L. Duò, B. Hecht, M. Finazzi, and G. Cerullo, "Dynamics of four-photon photoluminescence in gold nanoantennas," Nano Lett. **12**, 2941 (2012).
[33]V. V. Lozovoy, I. Pastirk, K. A. Walowicz, and M. Dantus, "Multiphoton intrapulse interference. II. Control of two- and three-photon laser induced fluorescence with shaped pulses," J. Chem. Phys. **118**, 3187 (2003).
[34]N. Accanto, P. M. de Roque, M. Galvan-Sosa, I. M. Hancu, and N. F. van Hulst, "Selective excitation of individual nanoantennas by pure spectral phase control," New J. Phys. Focus issue on Nanoscale Quantum Optics (2018).